

## 500W Circular Coil Parameters Mathematical Design for Wireless Power Transfer with Ferrite Core

<https://doi.org/10.3991/ijim.v16i11.30097>

Nadia Nazieha Nanda<sup>(✉)</sup>, Nur Shahida Midi, Siti Hajar Yusoff,  
Ahmed Samir Abed Badawi  
Electrical and Computer Engineering Department, International Islamic University Malaysia,  
Kuala Lumpur, Malaysia  
nnazieha.nanda@gmail.com

**Abstract**—The efficiency of wireless pad designs with ferrite cores has been established in several investigations. However, they seldom offered a viable solution to the problem of modifying the ferrite form's geometric shape. The use of a ferrite core in the primary and secondary coils has been suggested by several researchers. The ferrite core design, on the other hand, is still in the works. Using the wrong ferrite core design might result in unnecessary extra weight and higher production costs. The circular coil design in the primary and secondary for wireless power transfer (WPT) in electric vehicles is studied in this research. The suggested coil design is used to develop mathematical design utilizing numerical solutions. Later, using Multisims software, this coil design is produced in simulation. The suggested coil design's power efficiency is examined and contrasted between computed and simulated results. Finally, based on the results of the power efficiency, a definitive discussion is presented.

**Keywords**—electric vehicle (EV), numerical, mathematical, coil design, circular, wireless power transfer (WPT)

### 1 Introduction

In a wireless power transfer system, the coupling power transmission idea is utilised to transport electric power from the transmitter coil to the receiver coil beneath the electric vehicle (EV) chassis [1–2]. Capacitive wireless power transfer (CWPT) and inductive wireless power transfer (IWPT) are two types of wireless power transmission (WPT) [3–7].

The coupling of two coils produces an electric field, which is the basis of CWPT. The generated voltage from the transmitter coil produces an electromagnetic field, which creates an electrostatic field on the receiver coil [8]. The connection of the transmitter and receiver coils in the IWPT, on the other hand, creates an electric field. Ampere's Law and Faraday's Law [9] are responsible for the magnetic field created.

Most researchers have attempted to identify the way to charge the EV by using the wireless concept several years back [10–11]. Inductive charging, as depicted in Figure 1, is viewed as the most suitable alternative for finding a sustainable solution to petroleum

depletion where electromagnetic coupling generates electricity. This cutting-edge technology enables the EV to charge securely and without the use of cables. The public energy grid is connected to a transmitter coil. Electricity passes through the transmitter coil as soon as the driver starts charging, generating a magnetic field [12].

An electric current flows via the receiver coil, which is placed beneath the EV chassis, as a result of the magnetic field. Induced electricity is used to charge the batteries of electric vehicles [13].

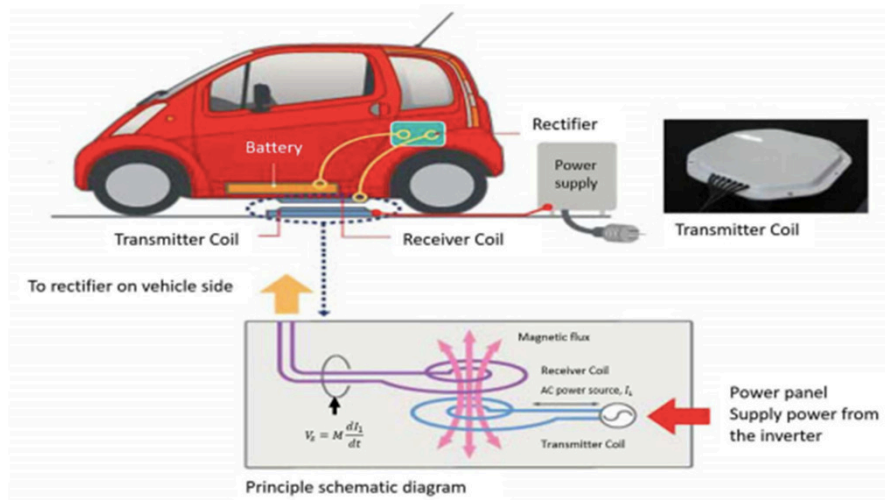


Fig. 1. Wireless battery charging system in EV [12]

For the wireless charging of electric vehicles, a variety of coil configurations are available. The most frequent designs are circular pads [1], [4], [10], [12], rectangular pads [1], [12], [13], Double-D pads [11], [14], and Double-D pads [1]. In this work, the circular coil pair design is the sole topic of discussion. The following is how it's laid out: Section II describes the project's approach, while Section III includes mathematical and numerical solutions as well as Multisims simulation data. Finally, the essay draws to a close in Section IV.

## 2 Methodology

In order to transfer power wirelessly, energy is delivered from the primary side to the secondary side without any physical contact [16]. As the power transfer mechanism, the core magnet component generates this magnetic field.

This section will provide a summary of the methodologies employed throughout the research. This approach is divided into main two parts, one for coil parameter calculations and the other for simulation. The coil parameters will be determined first, and the calculated and simulated power at both primary and secondary plates will be compared.

The coupling coefficient ( $k$ ) of the coil pair determines the IWPT capabilities, which is controlled by the coil structure, also known as coil geometric design [17]. The transmitted power from the transmitter coil to the reception coil is used in the IWPT circuit.

A magnetic field is created between the transmitter coil  $L_p$  and the reception coil  $L_s$  [18–19]. The mutual inductance,  $M$ , increases as the coupling coefficient ( $k$ ) increases, increasing the power transfer. Changes in  $k$  have an impact on the output power. The coupling coefficient must be less than or equal to the critical coupling coefficient. ( $k < k_c$ ), the most optimum  $k$  is chosen, as shown in Figure 2 [20–21].

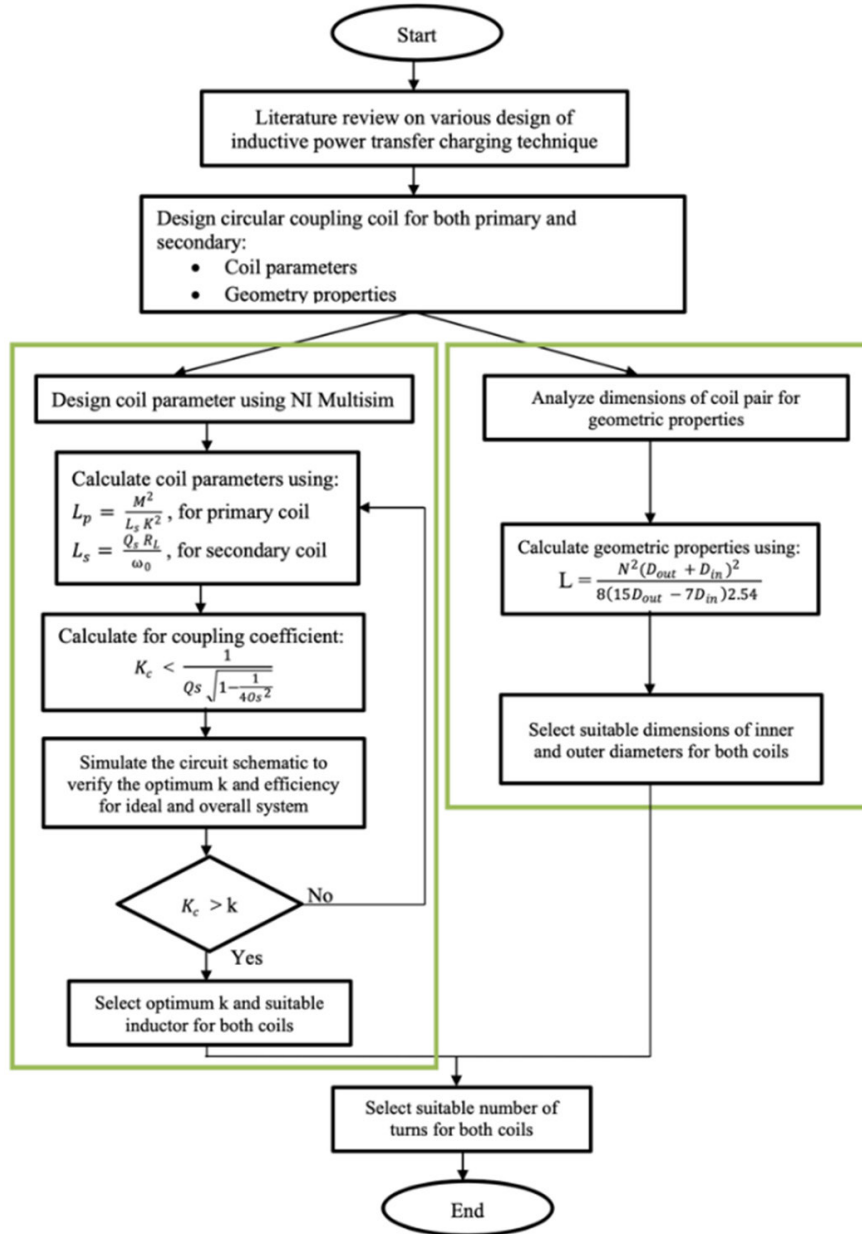


Fig. 2. The proposed methodology flowchart

Based on the proposed methods in Figure 2, the geometry characteristics for primary and secondary coils are calculated. The following is an example of the basic notion of a WPT schematic circuit, as shown in Figure 3. This circuit is in ideal work conditions order, which means it has no internal resistance ( $R_p = R_s = 0$ ). The schematic circuit for WPT is built using the simulation software NI Multisim, which is listed below.

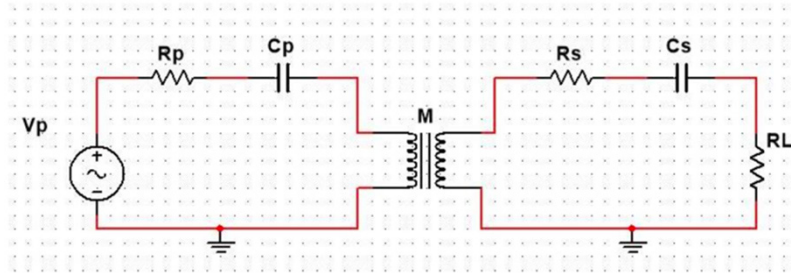


Fig. 3. Basic concept of WPT schematic circuit

The proposed 500W circular coil parameters needed to construct the schematic circuit are summarised in Table 1 below.

Table 1. Coil parameters needed

Primary voltage	$V_p$
Secondary voltage	$V_s$
Primary capacitance	$C_p$
Secondary capacitance	$C_s$
Primary resistance	$R_p$
Secondary resistance	$R_s$
Load resistance	$R_L$
Primary inductance	$L_p$
Secondary inductance	$L_s$
Mutual inductance	$M$
Coupling coefficient	$k$

When designing the transmitter and receiver coils for the proposed coil pair, the required self-inductance of each inductance coil is given by equation (1) and equation (2).  $L_p$  refers to the transmitter self-inductance, whereas  $L_s$  refers to the receiver self-inductance. To continue the calculation procedure, the values of receiver quality factor,  $Q_s$ , operating frequency in 0, mutual inductance,  $M$ , and coupling coefficient,  $k$  must be determined before the requisite self-inductance for both transmitter and receiver coils can be calculated. The quantity of inductance that connects the transmitter coil to its neighbouring coil, the receiver coil, is denoted by  $M$ . The strength of  $M$  can be affected by the distance between the two inductance coils. Equation is used to find value of  $M$ . (3) as shown below:

$$L_p = \frac{M^2}{L_s k^2} \quad (1)$$

$$L_s = \frac{Q_s R_L}{\omega_o} \quad (2)$$

$$M = \frac{I_{s,rms} R_L}{I_{p,rms} \omega_o} \quad (3)$$

Equation (4) is used to compute the load resistance, whereas equation (5) is used to get the essential coupling coefficient,  $k_c$ . The value of the coupling coefficient,  $k$ , should be less than the value of the critical coupling coefficient,  $k_c$ , for a bifurcation-free operation, ( $k < k_c$ ). To pick the appropriate  $k$  for the coil coupling, use equation (5) below to calculate the appropriate critical coupling coefficient,  $k_c$ .

$$R_L = \frac{(V_o)^2}{P_o} \quad (4)$$

$$k_c < \frac{1}{Q_s \sqrt{1 - \frac{1}{4Q_s^2}}} \quad (5)$$

Equations (6) and (7) may be used to compute the RMS values of current in the primary and secondary sides:

$$I_{p,rms} = \frac{P_o}{V_p} \quad (6)$$

$$I_{s,rms} = \frac{V_o}{R_L} \quad (7)$$

The validity of the parameters is validated by simulating the ideal outcome; if the power on the primary and secondary sides is the same, there is no internal or external resistance. Running the NI Multisim software will give the current and voltage values. Equation (8) can be used to compute power on both the primary and secondary sides.

$$P = V \cdot I \quad (8)$$

Four pairs of circular coils have been proposed for this study. The recommended coil will either be ferrite-free or contain ferrite. If ferrite is available, the preferred coil will be either double in-phase or double out-phase. The proper number of turns for the primary and secondary coils will be computed in the next section, which dives into the mathematical design of the coil characteristics. Table 2 shows a summary of the suggested coil designs.

**Table 2.** Primary and secondary coil proposed designs

Pair	Primary Coil Designs	Secondary Coil Designs
1	Ferrite-less	Ferrite-less
2	With double ferrites	Ferrite-less
3	With double ferrites (in-phase)	Ferrite-less
4	With double ferrites (out-phase)	Ferrite-less

### 3 Results

#### 3.1 Numerical solutions for coil parameters

This model is based on a 500 W operation with a resonance frequency of 40 kHz and a voltage output of 48 V.

Below is the numerical solution for the proposed coil parameters. This mathematical computation begins by determining the ideal circuit's inductance and capacitance values.

$$P_o = 500 \text{ W}; V_p = 120 \text{ V}; V_o = 48 \text{ V}; f = 40 \text{ kHz}$$

$$\omega_o = 2\pi(40k) = 251327.41 \frac{\text{krad}}{\text{s}} \quad (9)$$

$$R_L = \frac{(V_o)^2}{P_o} = \frac{(48)^2}{500} = 4.6 \Omega \quad (10)$$

Where  $Q_s = 4$  is specified; using equation (11) below, calculate an appropriate coupling coefficient:

$$k_c < \frac{1}{Q_s \sqrt{1 - \frac{1}{4Q_s^2}}}, k_c < 0.248 \quad (11)$$

The value of  $k_c$  derived from the computation is 0.248. As a result, the value of  $k$  is chosen to be 0.2 as it must be smaller than  $k_c$ .

$$I_{p,rms} = \frac{P_o}{V_p} = \frac{150}{120} = 4.167 \text{ A} \quad (12)$$

$$I_{s,rms} = \frac{V_o}{R_L} = \frac{48}{4.6} = 10.435 \text{ A} \quad (13)$$

$$L_s = \frac{Q_s R_L}{\omega_o} = \frac{4(4.6)}{251327.41} = 73.211 \mu\text{H} \quad (14)$$

$$M = \frac{I_{s,rms} R_L}{I_{p,rms} \omega_o} = \frac{(10.435)(4.6)}{(4.167)(251327.41)} = 45.834 \mu H \quad (15)$$

$$L_p = \frac{M^2}{L_s k^2} = \frac{45.834 \mu^2}{(73.211 \mu)(0.2)^2} = 716.363 \mu H \quad (16)$$

$$\omega_o = \frac{1}{2\pi \sqrt{L_s C_s}}, C_s = 216.244 nF \quad (17)$$

$$\omega_o = \frac{1}{2\pi \sqrt{L_p C_p}}, C_p = 22.100 nF \quad (18)$$

The list of parameters obtained from these equations are summarised in Table 3.

**Table 3.** Circuit parameters

Parameters	Values
$V_{p,rms}$	120 V
$V_{s,rms}$	48 V
$I_{p,rms}$	4.167 A
$I_{s,rms}$	10.4 A
$R_L$	4.6 $\Omega$
$L_p$	716.363 $\mu H$
$L_s$	73.211 $\mu H$
$M$	45.834 $\mu H$
$C_p$	22.100 nF
$C_s$	216.244 nF

### 3.2 Simulation results discussion

Equations (19) and (20) showed a comparison of computed and simulated values for the schematic circuit simulation in NI Multisims software.

$$\text{Efficiency, } \eta = \frac{\text{Power}_{received}}{\text{Power}_{transmitted}} \times 100\% \quad (19)$$

$$\text{Simulated, Efficiency} = \frac{479.25}{493} \times 100\% = 99.4\% \quad (20)$$

Figure 4 and Figure 5 showed the bar graph of the calculated and simulated primary and secondary voltages and currents.

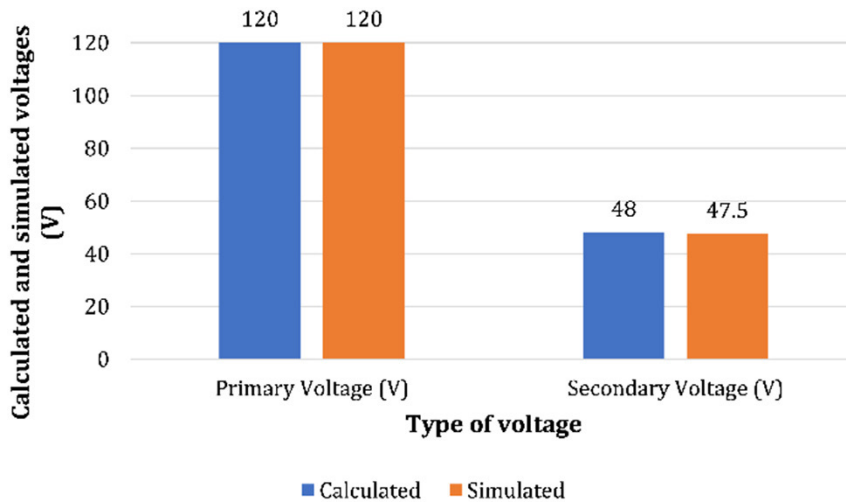


Fig. 4. Differences in primary and secondary voltages computed and simulated

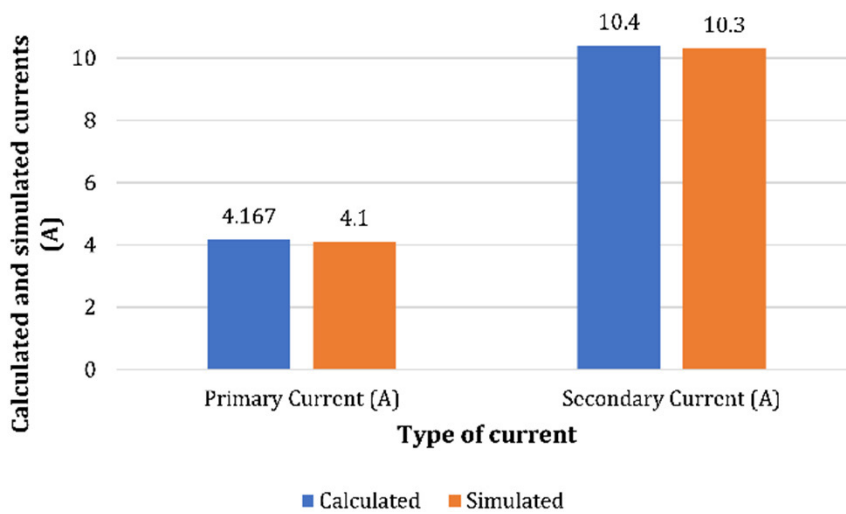


Fig. 5. Differences in primary and secondary currents computed and simulated

The differences between the calculated and simulated values of the system circuit are quite modest, as shown in Figures 4 and 5. Because the differences are very small, the results may be trusted to be further investigated. The findings are then analysed further to determine the transmitted and received power. The efficiency percentages for transmitted and received power are summarised in Figure 6, and the bar graph of the power analyses is depicted in Figure 7.

Because this circular coil is meant to have a 500 W output power, the calculated transmitted and received power are predicted to be 500 W. In practise, though, it is natural to experience a loss of efficiency. The results were summarised in Figures 6 and 7.

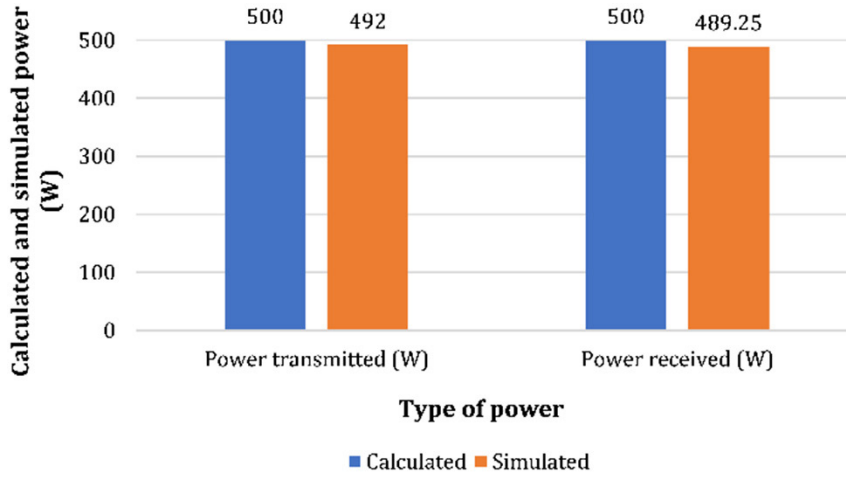


Fig. 6. Differences in power transmitted and received computed and simulated

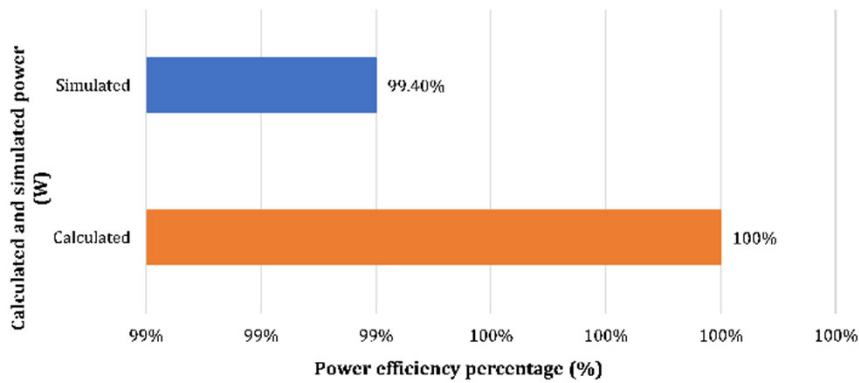


Fig. 7. Differences in power efficiency percentages calculated and simulated

In a perfect circumstance, there would be no internal resistance, therefore the power transfer efficiency would be 100%. When comparing the calculated and simulated data, it can be inferred that the efficiency of the simulated circuit is 99.4%.

### 3.3 Numerical analysis

Primary and secondary coil geometry properties:

$$L = \frac{N^2(D_{out} + D_{in})^2}{8(15D_{out} - 7D_{in})2.54} \quad (21)$$

For circular coil diameter design,

$$716.363 = \frac{N_p^2 (30.0 + 10.0)^2}{8(15(30.0) - 7(10.0))2.54}, N_p = 58.8 \approx 58 \text{ turns} \quad (22)$$

$$73.211 = \frac{N_s^2 (30.0 + 10.0)^2}{8(15(30.0) - 7(10.0))2.54}, N_s = 18.8 \approx 18 \text{ turns} \quad (23)$$

Table 4 summarises the primary and secondary parameters employed in the proposed circular coil design. The circular coil on the transmitter side (primary coil) is varied with four distinct ferrite variants for this research. Meanwhile, for the four primary coil modifications, the circular coil on the receiver side (secondary coil) remains the same.

**Table 4.** Summary of calculated geometry properties

Coil	Dimensions		Number of turns (N)	Number of ferrites
	Inner Diameter (cm)	Outer Diameter (cm)		
Primary Coil (P <sub>1</sub> )	10.0	30.0	58	None
Primary Coil (P <sub>2</sub> )				2
Primary Coil (P <sub>3</sub> )				2 (double), in phase
Primary Coil (P <sub>4</sub> )				2 (double), out phase
Secondary Coil	10.0	30.0	18	None

The transmitted power may be monitored by altering the primary coil, and the most suitable suggested primary coil can then be selected as the most compatible primary coil to couple with the proposed secondary coil. The magnetic flux density of the findings may be determined using the JMAG Designer software or any other compatible software. The magnetic flux density assessments of the suggested circular coil design will not be detailed in this paper.

## 4 Conclusion

The inner and outer diameters, as well as the number of turns necessary for both the main and secondary coils, were calculated using the inductance values. NI Multisims software was used to build the circuit diagram. The design overview was supplied, which included all of the dimensions and number of turns. According to calculations, the transmitted power efficiency from the primary coil to the secondary coil is just 0.6% loss. As a consequence, the new recommended coil has a power efficiency of 99.4%, making this research a success.

## 5 Acknowledgement

This work was partially supported under IIUM-UMP-UITM SUSTAINABLE RESEARCH COLLABORATION GRANT 2020 (SRCG) number SRCG20-049-0049.

## 6 References

- [1] A. Zaini, S. H. Yusoff, A. A. Abdullah, S. Khan, F. A. Rahman, and N. N. Nanda, "Investigation of magnetic properties for different coil sizes of dynamic wireless charging pads for electric vehicles (EV)," *IJUM Eng. J.*, vol. 21, no. 1, pp. 23–32, 2020, <https://doi.org/10.31436/iiumej.v21i1.1108>
- [2] K. Aditya, "Design and Implementation of An Inductive Power Transfer System for Wireless Charging of Future Electric Transportation," 2016.
- [3] R. Bosshard and J. W. Kolar, "Inductive Power," no. September, pp. 22–30, 2016, <https://doi.org/10.1109/VTC.1979.1622664>
- [4] S. Kim, G. A. Covic, and J. T. Boys, "Tripolar pad for inductive power transfer systems for EV charging," *IEEE Trans. Power Electron.*, vol. 32, no. 7, pp. 5045–5057, 2017, <https://doi.org/10.1109/TPEL.2016.2606893>
- [5] M. Bojarski, E. Asa, K. Colak, and D. Czarkowski, "Analysis and control of multiphase inductively coupled resonant converter for wireless electric vehicle charger applications," *IEEE Trans. Transp. Electrification*, vol. 3, no. 2, pp. 312–320, 2017, <https://doi.org/10.1109/TTE.2016.2566921>
- [6] J. P. K. Sampath, D. M. Vilathgamuwa, and A. Alphones, "Efficiency enhancement for dynamic wireless power transfer system with segmented transmitter array," *IEEE Trans. Transp. Electrification*, vol. 2, no. 1, pp. 76–85, 2016, <https://doi.org/10.1109/TTE.2015.2508721>
- [7] J. M. Miller and A. Daga, "Elements of wireless power transfer essential to high power charging of heavy duty vehicles," *IEEE Trans. Transp. Electrification*, vol. 1, no. 1, pp. 26–39, 2015, <https://doi.org/10.1109/TTE.2015.2426500>
- [8] S. A. Zaini, S. H. Yusoff, M. S. Abu Hanifah, E. Sulaiman, N. N. Nanda, and S. H. Badruhisam, "Design of circular pad coupler of inductive power transfer for electric vehicle (EV)," in *8th International Conference on Computer and Communication Engineering (ICCCCE)*, 2021, vol. 2020, pp. 202–207. <https://doi.org/10.1109/ICCCCE50029.2021.9467228>
- [9] K. Aditya, V. K. Sood, and S. S. Williamson, "Magnetic characterization of unsymmetrical coil pairs using archimedean spirals for wider misalignment tolerance in ipt systems," *IEEE Trans. Transp. Electrification*, vol. 3, no. 2, pp. 454–463, 2017, <https://doi.org/10.1109/TTE.2017.2673847>
- [10] G. A. Covic and J. T. Boys, "Inductive power transfer," *Proc. IEEE*, vol. 101, no. 6, pp. 1276–1289, 2013, <https://doi.org/10.1109/JPROC.2013.2244536>
- [11] N. N. Nanda, S. H. Yusoff, S. F. Toha, N. F. Hasbullah, and A. S. Roszaidie, "A brief review: basic coil designs for inductive power transfer," *Indones. J. Electr. Eng. Comput. Sci.*, vol. 20, no. 3, p. 1703, 2020, <https://doi.org/10.11591/ijeecs.v20.i3.pp1703-1716>
- [12] P. S. R. Nayak and D. Kishan, "Performance analysis of series/parallel and dual side LCC compensation topologies of inductive power transfer for EV battery charging system," *Front. Energy*, pp. 1–14, 2018, <https://doi.org/10.1007/s11708-018-0549-z>
- [13] S. Yusoff, L. De Lillo, P. Zanchetta, and P. Wheeler, "Predictive Control of a direct AC/AC matrix converter power supply under non-linear load conditions," *15th Int. Power Electron. Motion Control Conf. Expo. EPE-PEMC 2012 ECCE Eur.*, pp. 3–8, 2012, <https://doi.org/10.1109/EPEPEMC.2012.6397340>
- [14] C. Liu, "Overview of Coil Designs for Wireless Charging of Electric Vehicle," pp. 15–18, 2017. <https://doi.org/10.1109/WoW.2017.7959389>
- [15] M. Mohammad and S. Choi, "Optimization of ferrite core to reduce the core loss in double-D pad of wireless charging system for electric vehicles," *Conf. Proc.—IEEE Appl. Power Electron. Conf. Expo.—APEC*, vol. 2018-March, pp. 1350–1356, 2018, <https://doi.org/10.1109/APEC.2018.8341192>

- [16] A. Ahmad, "A comprehensive review of wireless charging technologies for electric vehicles," vol. 7782, no. c, 2017, <https://doi.org/10.1109/TTE.2017.2771619>
- [17] U. K. Madawala and D. J. Thrimawithana, "A bidirectional inductive power interface for electric vehicles in V2G systems," *IEEE Trans. Ind. Electron.*, vol. 58, no. 10, pp. 4789–4796, 2011, <https://doi.org/10.1109/TIE.2011.2114312>
- [18] L. Strauch, M. Pavlin, and V. B. Bregar, "Optimization, design, and modeling of ferrite core geometry for inductive wireless power transfer," *Int. J. Appl. Electromagn. Mech.*, vol. 49, no. 1, pp. 145–155, 2015, <https://doi.org/10.3233/JAE-150029>
- [19] S. Djuric, G. Stojanovic, M. Damnjanovic, M. Radovanovic, and E. Laboure, "Design, modeling, and analysis of a compact planar transformer," vol. 48, no. 11, pp. 4135–4138, 2012. <https://doi.org/10.1109/TMAG.2012.2202642>
- [20] S. H. Yusoff, N. N. Nanda, N. S. Midi, and A. S. Abed Badawi, "Mathematical Design of Coil Parameter for Wireless Power Transfer using NI Multisims Software," in *8th International Conference on Computer and Communication Engineering (ICCCCE)*, 2021, pp. 99–103. <https://doi.org/10.1109/ICCCCE50029.2021.9467166>
- [21] A. A. Abdullah *et al.*, "Design of U and I Ferrite Core On Dynamic Wireless Charging for Electric Vehicle," in *8th International Conference on Computer and Communication Engineering (ICCCCE)*, 2021, pp. 104–109. <https://doi.org/10.1109/ICCCCE50029.2021.9467217>
- [22] W. Zheng, and J. Liu, "Hybrid sliding mode control technology of electric vehicle based on wireless sensor," *International Journal of Online Engineering (IJOE)*, vol. 13, no. 05, p. 97, 2017. <https://doi.org/10.3991/ijoe.v13i05.7052>
- [23] M. Han, "Application of artificial intelligence detection system based on multi-sensor data fusion," *International Journal of Online Engineering (IJOE)*, vol. 14, no. 06, p. 31, 2018. <https://doi.org/10.3991/ijoe.v14i06.8696>
- [24] F. Hussein, L. ben Aissa, A. Abdalla Mohamed, I. Alruwaili, S. and A. Alanzi, "Development of a secured vehicle spot detection system using GSM," *International Journal of Interactive Mobile Technologies (IJIM)*, vol. 15, no. 04, p. 85, 2021. <https://doi.org/10.3991/ijim.v15i04.19267>

## 7 Authors

In June 2019, **Nadia Naziha Nanda** graduated from the International Islamic University Malaysia (IIUM) with a bachelor's degree in Communication Engineering. In addition, she graduated with a Master of Science majoring in Computer and Information-Electronics Engineering in October 2021 from the same university. She worked on multiple coil pair geometries for inductive wireless power transfer, which included designing the coil pairs as well as their magnetic coupling. Her research includes using the Multisims software to simulate the coil pairs design and the JMAG Designer software to calculate the magnetic flux density of the designed coil pairs. Her area of interest is coupling coil and power transmission efficiency. She currently works as the Structural Design Engineer (GT) at Intel.

**Nur Shahida Midi** received a M.Eng degree in Electrical and Electronic System from Tokai University, Japan and a Ph.D degree from Tokai University, Japan, in 2012 and 2015 respectively. She has been appointed as Assistant Professor in Department of Electrical and Computer Engineering, Faculty of Engineering, International Islamic University Malaysia (IIUM). Her current research interests include high voltage

phenomenon, energy harvesting, power management, Internet of Things (IoT), and waste management. E-mail: [nurshahida@iium.edu.my](mailto:nurshahida@iium.edu.my)

**Siti Hajar Yusoff** received the M.Eng. degree in electrical engineering (First Class Honors) and a PhD degree in electrical engineering from the University of Nottingham, UK, in 2009 and 2014, respectively. In 2015, she became an Assistant Professor in the Department of Electrical and Computer Engineering at International Islamic University Malaysia, Gombak. She is now a lecturer in control of power electronics systems and electrical power systems. Her research interests include control of power converters and drives, Matrix and multilevel converters, IoT, smart meter, wireless power transfer for dynamic charging in electric vehicles (EVs), and renewable energy. E-mail: [sitiyusoff@iium.edu.my](mailto:sitiyusoff@iium.edu.my)

**Ahmed Badawi** received his PhD in International Islamic University Malaysia (IIUM). His study is about maximum power point tracking for small scale wind turbine under Electrical Engineering. Badawi have finished his Master degree in Wind Energy, Control Dept. (2013) and B.Sc. Electrical Engineering Communication & Control Dept. (08th June, 2010) from Islamic University of Gaza, Gaza, Palestine. E-mail: [ab1005100@gmail.com](mailto:ab1005100@gmail.com)

Article submitted 2022-02-02. Resubmitted 2022-03-04. Final acceptance 2022-03-04. Final version published as submitted by the authors.